MINERALOGICAL MAGAZINE, DECEMBER 1985, VOL. 49, PP. 655–62

The partial melting of basalt and its enclosed mineral-filled cavities at Scawt Hill, Co. Antrim

D. E. KITCHEN

Department of Environmental Studies, University of Ulster, Jordanstown, Co. Antrim, Northern Ireland BT37 0QB

ABSTRACT. Partially melted basalts enclosing amygdales which have been completely melted formed at Scawt Hill adjacent to a Tertiary dolerite plug. Melting of the basalts commenced in a clay-rich mesostasis to produce a feldspathic liquid which then crystallized to an assemblage of dendritic olivine, skeletal hypersthene, opaque oxide and Mg-hercynite in a microcrystalline plagioclase matrix. An original mineral assemblage of zeolite, calcite, and saponite-nontronite in the amygdales melted and quenched to a brown glass now containing complexly zoned pyroxenes with plagioclase and opaque oxide. Melting commenced between 700–800 °C, reaching a maximum temperature of 1168 °C, and was followed by rapid cooling. The assimilation of remelted basalt may alter the course of crystallization of contaminated magmas.

KEYWORDS: basalts, melting, amygdales, Scawt Hill, Co. Antrim, Northern Ireland.

THE Tertiary dolerite plug at Scawt Hill, Co. Antrim, is best known for its associated metamorphism of Cretaceous chalk and flint (Tilley and Harwood 1931). Tertiary basaltic lavas overlying the chalk are also cut by the plug, and show evidence of recrystallization and partial melting. A selection of samples collected along a lava flow escarpment towards the plug on the north side (fig. 1) were observed to lose their basaltic texture progressively to within a metre of the contact where the rocks became indurated, and almost glassy in hand specimen. This paper considers the physical processes involved in melting, the evolution of the resultant textures, and outlines the wider implications of the remelting of basalt in the British Tertiary Volcanic Province.

Petrography of the basalts and dolerites

The dolerite is a fresh aphyric rock with anhedral olivine (Fo 78–71) intergrown with normally zoned plagioclase (An 73–68), and colourless subophitic augite. The mesostasis consists of a fibrous zeolite (unidentified) and calcite.

Unaltered basalts. These lavas are olivine-phyric with anhedral, partially serpentinized olivine phenocrysts (Fo 81–65), enclosing spinel, and partially mantled by Ti-magnetite. Small entirely serpentinized olivines with magnetite, ilmenite, anhedral augite, and plagioclase (An 76–68) form a granular to subophitic groundmass with interstitial brown amorphous clay (saponite-nontronite) and zeolite in the mesostasis. Amygdales (1–5 mm) are lined with clay, calcite, and zeolite.

2 m from the contact the lavas have substantially recrystallized, and the clay-rich mesostasis has melted. Olivines (Fo 84–65) are partially serpentinized, and also partially recrystallized to microcrystalline hypersthene and olivine due to the metamorphism of an earlier generation of serpentine (fig. 2A). Augite is unchanged texturally, but shows peripheral compositional variation (below) due to reaction with a matrix melt. Plagioclase is euhedral where enclosed by augite, but elsewhere, after dissolution in the matrix melt, recrystallized to a microcrystalline mosaic around skeletal hypersthene and opaque oxide. Amygdales in these rocks have completely melted, and then partially recrystallized to produce coarse crystals of compositionally zoned pyroxene and plagioclase with Fe-Ti oxide in a dark brown glass.

Contact rocks. The rocks immediately adjacent to the contact are entirely recrystallized. A few remnant olivine phenocrysts do occur, but are substantially replaced by microcrystalline hypersthene and olivine (above). Metamorphism of the groundmass has produced a dark fine-grained to microcrystalline aggregate of olivine, hypersthene, plagioclase, magnetite and ilmenite. Irregular streaks and lenses of devitrified basalt melt a few millimetres wide and up to a few centimetres long enclose dendritic olivine, microcrystalline bronzite–hypersthene, skeletal magnetite, ilmenite and Mg-hercynite in a cryptocrystalline plagioclase matrix (fig. 2). Amygdales, so common in the unaltered basalt, are absent from these rocks. As some signs of

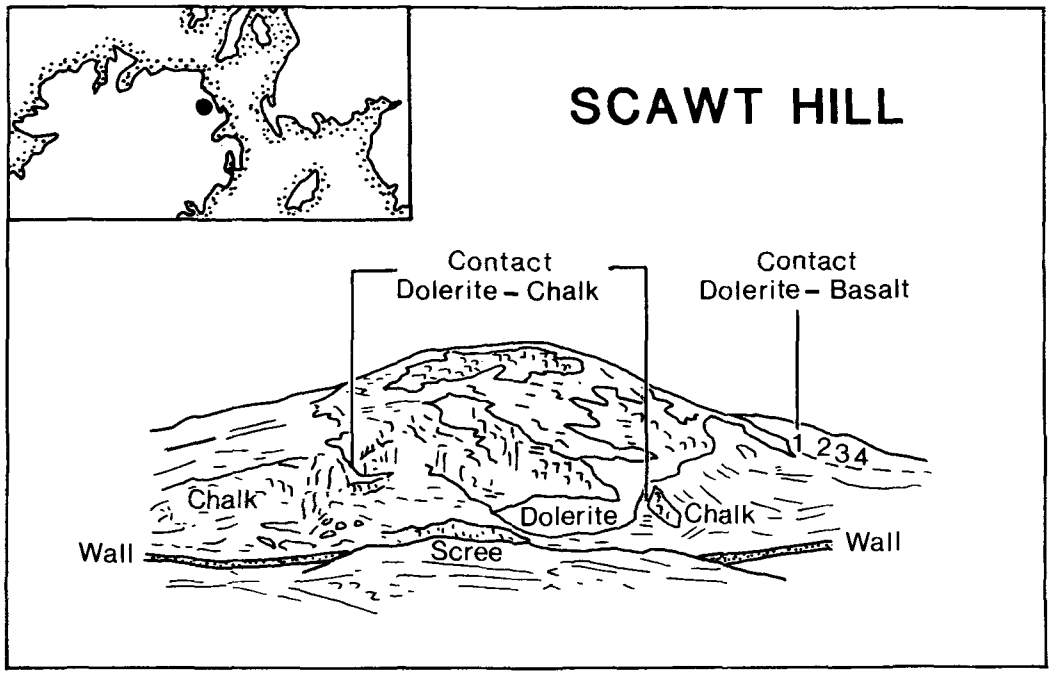

FIG. 1. Location map and field sketch (with permission J. Preston).

plastic deformation were observed in thin section, it is possible that original amygdales became melted, deformed, and dispersed in the surrounding basaltic melt.

Bulk rock analyses

Two fresh and two metamorphosed rocks were collected from the same flow approaching the contact (Table I). Compositional variation between samples is limited, and easily explained by variation in modal olivine and slight secondary alteration prior to metamorphism (Agrell and Langley, 1955). A sample of dolerite adjacent to the contact shows no sign of bulk or selective contamination by the basalt.

Basalt mineralogy

Unaltered basalt. Compositional trends for olivine, pyroxene, and plagioclase (Table II) are typical of Tertiary olivine basalts from Antrim (Lyle, 1984, pers. comm.). The brown saponite-nontronite mesostasis (Table I) is ol-, hy- and co-normative with a composition that plots well away from the 1 kbar basalt eutectic, thus representing a highly altered residual glass (fig. 3).

2 m from the contact. Recrystallized olivine and plagioclase are similar in composition to groundmass phases in the unaltered basalt. Augite, however, shows peripheral alteration to hypersthene as a consequence of reaction with the melted clay-rich mesostasis (fig. 4, Table II). Magnetite and ilmenite (Table III) show only limited compositional variation between samples. Variation in magnetite from a Cr- to Ti-rich variety is due to reaction of an original Cr-spinel with the basaltic magma prior to metamorphism (Ridley, 1973).

Contact rocks. Mineral compositions in the rheomorphic segregations show variation relative to surrounding recrystallized basalt. Olivines are richer in Al and Ca reflecting the high activity of these elements in the feldspathic melt. Hypersthene (fig. 4, Table II) is more Mg-rich than surrounding

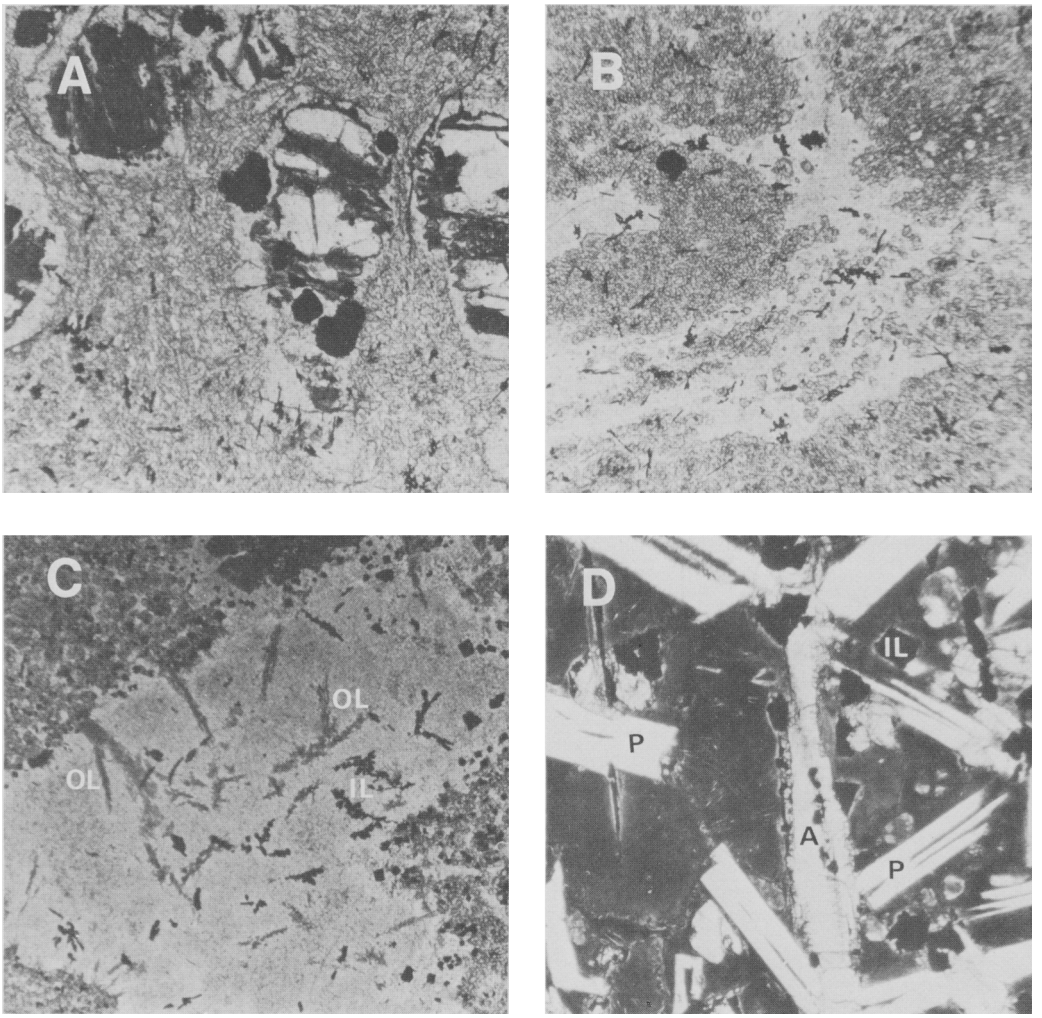

FIG. 2. A. 2 m from the contact. Olivine phenocrysts in recrystallized basalt. Note the mantle of microcrystalline hypersthene and olivine replacing serpentine formed prior to metamorphism. B. Metamorphosed basalt at the contact. Note the light coloured areas of devitrified feldspathic glass containing microlites of hypersthene and ilmenite surrounded by recrystallized basalt matrix. C. Metamorphosed basalt at the contact. Note the skeletal olivine (OL) and ilmenite (IL) in clear devitrified feldspathic melt. D. Metamorphosed amygdale, 2 m from the contact. Note the skeletal plagioclase (P), augite (A), and ilmenite (Il) in dark glass. Field of view 2 mm in each photograph.

matrix hypersthene, possibly reflecting a higher oxygen fugacity in the segregated basalt melt (Kitchen, 1984). Cryptocrystalline plagioclase in the devitrified melt and surrounding recrystallized basalt overlap in composition. Dark brown areas in the cryptocrystalline plagioclase, however, contain up to 3.64% FeO, 2.02% MgO, and 0.37% TiO_2, and show some evidence of coupled replacement of Ca–Al by $Mg–Fe^{3+}$ at high Fe concentrations. High FeO concentrations have been reported from plagioclase experimentally grown in basaltic melts (Schiffman and Lofgren, 1981) and related to cooling rates in excess of 218 °C/h when Fe-entrapment occurs on the crystal interface in non-strochiometric proportions. Magnetite and ilmenite in the devitrified melt show some enrichment in Mg, Cr, and Al relative to the surrounding basalt (Table III).

Table I Major element, trace element and normative analyses of dolerite, basalt and glass.

	1	2	3	4	5	6	7	8	9
SiO_2	47.55	48.66	45.89	45.83	47.22	43.33	46.15	60.69	60.68
TiO_2	1.11	1.46	1.39	1.23	1.22	0.16	0.34	0.84	0.87
Al_2O_3	16.18	15.07	15.17	13.51	13.83	7.70	7.30	14.31	14.53
Fe_2O_3*	10.81	12.37	12.70	10.88	11.12	11.87†	14.89†	3.57†	2.40†
MnO	0.16	0.19	0.19	0.15	0.16	0.10	0.19	-	-
MgO	8.62	12.39	12.32	10.77	11.84	22.20	22.70	3.45	2.68
CaO	11.36	8.13	6.58	10.14	10.03	1.51	1.39	0.77	0.69
Na_2O	2.19	1.53	1.07	1.56	1.43	-	-	1.94	1.88
K_2O	0.35	0.28	0.27	0.16	0.11	-	-	8.71	9.99
P_2O_5	0.14	0.12	0.09	0.10	0.10	na	na	-	-
Total	98.47	100.20	95.67	94.33	97.06	86.87	92.96	94.28	93.72
PPM									
Rb	2	4	3	-	-	na	na	na	na
Sr	142	136	137	149	138	na	na	na	na
Ba	110	118	128	69	51	na	na	na	na
Zr	119	128	118	98	99	na	na	na	na
Ni	438	453	538	440	459	na	na	na	na
CIPW									
Q	-	-	-	-	-	-	-	6.89	5.05
co	-	-	1.37	-	-	4.95	4.77	-	-
or	2.07	1.59	1.59	0.95	0.65	-	-	51.5	59.08
ab	18.53	12.94	9.05	13.11	12.10	-	-	16.39	15.89
an	33.28	33.45	32.05	29.43	30.99	7.49	6.89	3.82	1.62
di	17.98	4.85	-	16.34	14.61	-	-	-	1.45
hy	10.29	33.99	42.43	20.73	25.66	66.66	72.49	13.78	8.97
ol	10.32	8.09	3.97	9.01	8.32	7.45	8.23	-	-
il	2.11	2.17	2.17	2.33	2.32	0.30	0.64	1.59	1.65
mt	3.56	2.77	2.64	2.17	2.17	-	-	-	-

1, dolerite : 2, fresh basalt : 3, fresh basalt : 4, basalt 2m from contact : 5, basalt at the contact. + all iron as Fe_2O_3, XRF analyses. 6, 7 brown mesostasis to basalt : 8, 9, glass in melted mineral-filled cavities.
† all iron as FeO, microprobe analyses. na, no analyses.

Table II Microprobe analyses of olivines and pyroxenes.

	1	2	3	4	5	6	7	8	9	10	11	12
SiO_2	37.62	37.27	35.17	37.23	51.13	50.48	49.70	51.67	52.47	52.12	50.12	51.39
TiO_2	-	-	-	-	0.85	0.50	0.64	0.40	0.69	0.42	0.35	0.72
Al_2O_3	-	-	-	1.94	3.02	2.41	1.39	4.37	1.67	0.73	0.39	1.23
FeO*	22.29	26.81	26.62	26.02	8.40	7.08	18.29	21.18	17.05	22.24	27.20	17.20
MnO	0.39	0.27	0.29	0.29	0.15	0.12	0.24	0.30	0.44	0.45	0.68	
MgO	37.96	34.86	37.07	31.17	13.83	14.39	15.88	16.32	24.51	18.64	15.02	13.26
CaO	0.43	0.15	0.14	1.39	22.39	23.02	11.96	5.42	1.60	4.61	5.02	16.11
Na_2O	-	-	-	-	-	-	-	-	-	-	-	-
K_2O	-	-	-	-	-	-	-	-	-	-	-	-
Total	98.96	99.36	99.29	98.04	99.82	98.00	98.10	99.86	98.31	99.20	98.78	100.36
Si	0.994	0.995	0.990	1.004	1.908	1.905	1.926	1.936	1.941	1.979	1.971	1.953
Ti	-	-	-	-	0.025	0.015	0.020	0.012	0.020	0.013	0.014	0.021
Al	-	-	-	0.062	0.134	0.107	0.064	0.194	0.073	0.033	0.018	0.056
Fe*	0.493	0.599	0.596	0.586	0.263	0.223	0.593	0.664	0.011	0.706	0.895	0.547
Mn	0.009	0.006	0.007	0.007	0.006	0.004	0.008	0.010	0.528	0.015	0.023	0.015
Mg	1.494	1.386	1.402	0.252	0.772	0.804	0.921	0.922	1.351	1.055	0.880	0.751
Ca	0.013	0.005	0.005	0.040	0.896	0.924	0.497	0.218	0.063	0.188	0.212	0.656
Na	-	-	-	-	-	-	-	-	-	-	-	-
K	-	-	-	-	-	-	-	-	-	-	-	-
O	4	4	4	4	6	6	6	6	6	6	6	6

Olivines: 1, dolerite; 2, fresh basalt; 3, 2m from contact; 4, in segregated melt. Pyroxene: 5, dolerite; 6, fresh basalt; 7, 2m from contact, 8, 2m from contact, 9, in segregated melt; 10-12, in glass in melted mineral-filled cavity.

Table III Microprobe analyses of opaque oxide phases and cryptocrystalline plagioclase.

	1	2	3	4	5	6	7	8	9	10
SiO_2	0.74	0.50	2.88	0.38	2.71	0.34	1.40	0.23	52.62	49.86
TiO_2	1.25	17.58	45.20	22.70	45.49	21.25	52.34	1.46	0.34	0.37
Al_2O_3	22.34	2.80	0.26	1.49	0.39	4.15	1.21	52.13	26.33	26.10
FeO*	32.19	63.66	40.31	63.56	42.94	56.21	38.15	28.93	1.69	3.64
MnO	0.65	0.35	1.20	0.37	0.30	0.46	0.33	0.15	-	-
MgO	8.05	2.38	1.27	1.81	4.05	3.54	5.07	11.99	0.67	2.02
Cr_2O_3	30.49	7.23	-	3.68	0.19	8.79	0.70	-	-	-
CaO	0.19	0.29	3.39	0.10	1.09	0.25	0.49	0.15	12.59	13.81
Na_2O	-	-	-	-	-	-	-	-	2.39	1.83
K_2O	-	-	-	-	-	-	-	-	3.28	2.11
Total	95.90	94.79	94.51	94.09	97.16	94.99	99.69	95.04	99.91	99.74
Si	0.026	0.021	0.075	0.016	0.069	0.014	0.034	0.054	2.435	2.337
Ti	0.032	0.533	0.889	0.693	0.886	0.614	0.937	0.256	0.013	0.014
Al	0.884	0.134	0.008	0.071	0.012	0.189	0.034	14.26	1.437	1.443
Fe	0.903	2.146	0.881	2.148	0.909	1.805	0.799	5.614	0.066	0.143
Mn	0.019	0.012	0.027	0.013	0.007	0.016	0.007	0.031	-	-
Mg	0.430	0.144	0.050	0.110	0.153	0.203	0.180	4.14	0.048	0.142
Cr	0.809	0.231	-	0.118	0.004	0.267	0.014	-	-	-
Ca	0.007	0.013	0.095	0.005	0.030	0.011	0.013	0.039	0.625	0.694
Na	-	-	-	-	-	-	-	-	0.215	0.168
k	-	-	-	-	-	-	-	-	0.189	0.123
O	4	4	3	4	3	4	3	32	8	8

1, spinel fresh basalt : 2, mgt. fresh basalt : 3 ilm. fresh basalt : 4 mgt. 2m from contact : 5 ilm. 2m from contact : 6 mgt. basalt melt : 7 ilm. basalt melt : 8 Mg-hercynite basalt melt : 9, 10 cryptocrystalline plagioclase, basalt melt.

* all iron as FeO. Low analytical totals in oxides can be corrected by assuming value for Fe 3+. Mgt = magnetite, ilm = ilmenite.

Petrography of the amygdales

The melted amygdales range in size from 5 mm to less than 1 mm, and contain a brown, partially devitrified glass with euhedral-subhedral crystals of pyroxene, plagioclase, and opaque oxide.

The pyroxenes are subhedral, prismatic, and colourless, ranging in size from 0.1–1 mm. Many examples have opaque oxide moulded around the crystal margin, but faces projecting into the glass have developed skeletal overgrowths. Multiple generations of plagioclase occur as euhedral lath-shaped crystals with skeletal terminations (An 55–36). These range in size from 0.1–1 mm and show an increasing tendency towards skeletal forms in the smaller crystals. Multiple generations of plagioclase have been related to undercooling of the melt with repeated nucleation at each jump in Δt, but may also occur with continuous cooling on variation of the cooling rate (Walker *et al.*, 1976; Lofgren, 1974). Subsequent partial devitrification of the glass produced a final generation of elongate, curved fibres of feldspar which proved too small to analyse. Skeletal crystals of Fe–Ti oxide contain exolved lamellae of Ti-magnetite and ilmenite, and are often surrounded by a border of colourless glass where the normally brown glass has lost its Fe to the opaque oxide.

Mineralogy of the amygdales

Pyroxenes. Three compositional trends are present in the pyroxenes: 1. Complex crystals of continuously zoned subcalcic augite to augite with small pigeonite cores; 2. Normally zoned pigeonite; 3. Normally zoned augite (fig. 5, Table II). All pyroxenes are related by a close correlation between Ca, Al, and Ti substitution (fig. 6), and most have a narrow border of Fe-enriched Ca-poor pyroxene of similar composition to skeletal forms in the glass. Similar compositional zoning observed after experimental studies on basalts has been related to rapid growth in structurally and compositionally complex melts (Walker *et al.*, 1976; Schiffman and Lofgren, 1981). Under such conditions the increase in Ti and Al concentration (fig. 6) has been related to high growth rates, and low diffusion rates accompanying rapid cooling. Tenuous analogy with the data of Schiffman and Lofgren (1981) suggests cooling rates in the order of

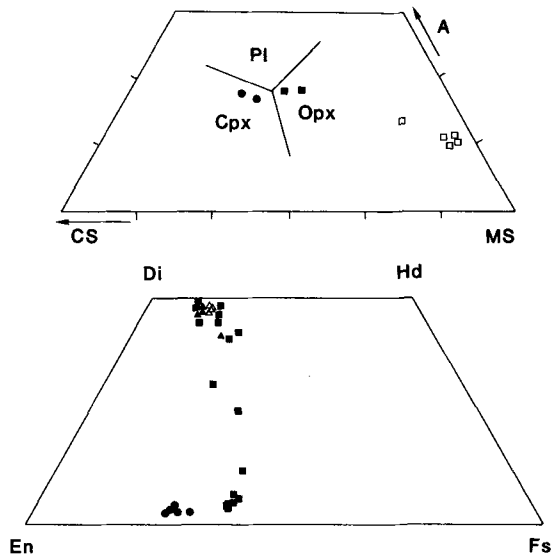

FIGS. 3 and 4. FIG. 3 (*above*). CMAS section at 1 kbar. Fresh basalts (circles); metamorphosed basalts (squares); clay mesostasis (open squares). FIG. 4 (*below*). Pyroxene quadrilateral showing the range in composition of pyroxenes from the Scawt Hill basalts. Basalt melt (circles); 2 m from contact (squares); fresh basalt (triangles); dolerite (open triangles).

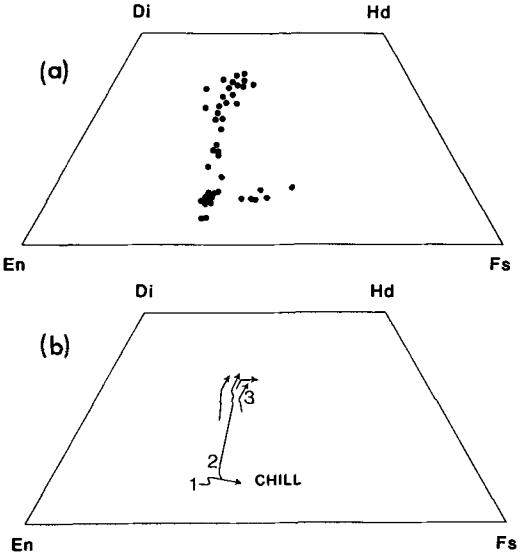

FIG. 5. Pyroxene quadrilateral diagrams showing (*a*) compositional range of pyroxene in the melted mineral-filled cavities, (*b*) individual zoning patterns. Numbers relate to fig. 6.

1–10 °C/h for the larger pyroxenes, and 84 °C/h for the Fe-rich skeletal crystals in the groundmass. Coarse subhedral textures in the amygdales contrast strongly with the microcrystalline and skeletal textures of surrounding basalt. Lofgren (1983) showed that the full range of textures produced by varying cooling rate can also be produced by varying the kind and density of heterogeneous nucleii at a constant cooling rate. The contrast in texture between basalt and enclosed amygdales may be explained by variable heterogeneous nucleation on submicroscopic unmelted remnants in liquids of contrasting structure and composition.

Glass compositions depend on the original proportion and composition of the infilling minerals. Generally they are metaluminous and rich in K_2O, Na_2O, FeO and MgO (Table I). The alkali elements show the greatest variation which may be related to initial zeolite composition, and the clay–zeolite ratio. Analytical totals (Table I) are presented on an anhydrous basis, but water contents were estimated to be around 6% on the basis of microprobe data.

Melting kinetics

Partial melting of the basalt commenced in the clay-rich mesostasis. The onset of melting is likely to have occurred above 750 °C when smectites and zeolites lose most of their constitutional water. The fine grain size, abundant water and alkalis from associated zeolite, will have resulted in rapid melting to produce a liquid in marked disequilibrium with the surrounding basalt. Microprobe analyses of the unaltered clay mesostasis suggest a strongly hy-normative liquid with low concentrations of alkalis. The addition of small amounts of zeolite may have locally produced liquids closer in composition to the coeval melts in the amygdales (Table I). Reaction of the matrix melt with surrounding basalt involved the dissolution of plagioclase, and addition of Ca derived from augite (above) to produce the highly feldspathic compositions observed in the rheomorphic segregations. Segregation of the melt into thin veins and lenses was accompanied by plastic deformation during which liquids from amygdales and basalt may have mixed. The maximum temperature at the contact is difficult to determine, but must have been in excess of 800–820 °C for the formation of olivine from serpentine around olivine phenocrysts (Deer *et al.*, 1975).

Melting of the amygdales would likewise have been a rapid process facilitated by the presence of water in the zeolite. Small areas of calcite in a few of the amygdales suggest a high partial pressure of carbon dioxide in addition to water. The behaviour of these amygdales on metamorphism contrasts

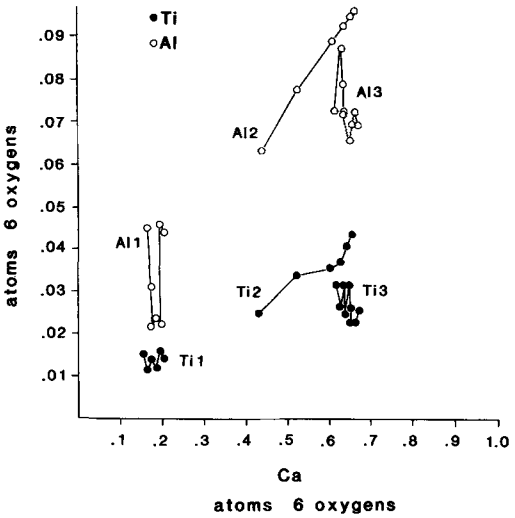

FIG. 6. This diagram illustrates examples of the correlation between Ca, Ti, and Al substitution in pyroxenes from the melted mineral-filled cavities: 1. individual pigeonite crystals; 2. continuously zoned crystal; 3. individual augite crystal. Scale = number of atoms to 6 oxygens.

with the solid-state recrystallization of amygdales in Tertiary lavas on Mull (Cann, 1965). The reason for this is uncertain, but must be related to compositional variation in the unaltered amygdales and the temperature of metamorphism. The application of mineral geothermometers to the complex melts in the amygdales must be open to question, but the two-pyroxene thermometer of Wells (1977) and the plagioclase melt method of Mathez (1973) suggest a temperature range of 1168–970 °C. These results are geologically reasonable, and compare favourably with the estimate of 936 °C for the dolerite solidus and 900 °C for the onset of quenching at the nearby plug of Tieveragh (Kitchen, 1984). At Scawt Hill the abundance of skeletal crystals in both the segregated rheomorphic melt and the amygdales show that melting was followed by a rapid quench. As discussed above, quench rates are difficult to determine due to the probable abundance of heterogeneous nucleii, but may have been in the order of 1–10 °C/h.

Discussion

Recent models for the early development of British Tertiary Volcanic centres involve the emplacement of intense complexes of sills and dykes (Thompson, 1982). Multiple injection of basaltic magma in such complexes has the potential to produce extensive partial melting of earlier basaltic rocks in addition to surrounding country rock (Kitchen, 1984). The melting and assimilation of unaltered basaltic rock will not effect the evolution of contaminated magmas; however, contamination by deuterically altered basalt can considerably alter the course of crystallization. In tholeiitic magmas the reworking of an acid mesostasis by partial melting would increase the proportion of residual granitic liquid. Assimilation of oxidized melts could produce the same effect by stimulating the crystallization of excess oxide minerals. In alkaline basalts the incorporation of hydrous melts rich in alkalis would likewise increase the proportion of final residue. At a later stage in the evolution of the central complexes, cauldron subsidence associated with high-level magma chambers offers a further opportunity for the assimilation of highly oxidized, hydrous rocks by the foundering of blocks of preheated incandescent lava. Outside the area of the British Tertiary Volcanic Province the interaction of upwelling basic magmas with their consolidated predecessors is of wide application elsewhere, in such settings as ocean ridges and islands. For example the contamination of basaltic melts by as little as 5% of acid residuum from earlier eruptions could substantially increase the proportion of rhyolitic magma on fractional crystallization of the contaminated melt.

Acknowledgements. I express my thanks to Dr John Preston for his help in preparing this paper, Jennifer Larkin for typing the manuscript and Mr Ian Alexander for preparing the diagrams. Part of this work was carried out during the tenure of a Northern Ireland Department of Education postgraduate studentship at the Queen's University Belfast.

REFERENCES

Agrell, S. O., and Langley, J. M. (1955) The dolerite plug at Tievbulliagh near Cushendall Co. Antrim. *Proc. R. Irish. Acad.* **59**, sect. B. 93–127.

Cann, J. R. 1965. The metamorphism of amygdales at S Airde Beinn northern Mull. *Mineral. Mag.* **34**, 92–106.

Deer, W. H., Howie, R. A., and Zussman, J. (1975) An introduction to the rock-forming minerals. Longmans, London.

Kitchen, D. E. (1984) Pyrometamorphism and the contamination of basaltic magma at Tieveragh, Co. Antrim. *J. Geol. Soc. London.* **141**, 733–45.

Lofgren, G. (1974) An experimental study of plagioclase crystal morphology. *Am. J. Sci.* **274**, 243–73.

——(1983) Effects of heterogeneous nucleation on basaltic textures: a dynamic crystallization study. *J. Petrol.* **24**, 229–55.

Mathez, P. (1973) Refinement of the Kudo-Weill plagioclase thermometer. *Contrib. Mineral. Petrol.* **41**, 66–72.

Ridley, W. I. (1973) The petrology of volcanic rocks from the Small Isles of Inverness-shire. *Rep. Inst. Geol. Sci.* London. 73–110.

Schiffman, P., and Lofgren, G. (1981) Dynamic crystallization studies on the Grande Ronde pillow basalts, Central Washington. *J. Geol.* **90,** 49–78.

Thompson, R. N. (1982) Magmatism of the British Tertiary Volcanic Province. Carnegie Review Article. *Scot. J. Geol.* **18,** 49–107.

Tilley, C. E., and Harwood, H. F. (1931) The dolerite-chalk contact at Scawt Hill, Co. Antrim. The production of basic alkaline rocks. *Mineral. Mag.* **22,** 439–68.

Walker, D., Kirkpatrick, R. J., Longhi, J., and Hays, J. F. (1976) Crystallization history of lunar picritic basalt sample 12002. Phase equilibria and cooling rate studies. *Geol. Soc. Am. Bull.* **87,** 646–56.

Wells, P. (1977) Pyroxene thermometry in simple and complex systems. *Contrib. Mineral. Petrol.* **62,** 129–39.

[*Manuscript received 5 December 1984; revised 18 March 1985*]